OFDM Based Visible Light Communication with Probabilistic Shaping

Tilahun Zerihun Gutema
tilahun.gutema@ed.ac.uk
Institute for Digital Communications
School of Engineering
The University of Edinburgh
Edinburgh, UK

Harald Haas
h.haas@ed.ac.uk
Institute for Digital Communications
School of Engineering
The University of Edinburgh
Edinburgh, UK

Wasiu O. Popoola
w.popoola@ed.ac.uk
Institute for Digital Communications
School of Engineering
The University of Edinburgh
Edinburgh, UK

ABSTRACT

A visible light communication (VLC) system using probabilistically shaped orthogonal frequency multiplexed (OFDM) modulation is presented. The average symbol energy of probabilistically shaped OFDM modulation is investigated for different modulation orders of quadrature amplitude modulation (QAM) under different entropy scenarios. Furthermore, the symbol error performance of the probabilistically shaped OFDM system under additive white Gaussian noise (AWGN) channel condition is evaluated. The probabilistically shaped OFDM system outperforms the uniformly distributed in the symbol error ratio performance. For 256-QAM with an entropy of 7.84 bits, we have shown a 3 dB gain in signal-to-noise ratio (SNR) per symbol compared to uniform 256-QAM at a symbol error ratio of 10^{-3}. This gain increases to 5.5 dB by decreasing the entropy to 6.80 bits.

CCS CONCEPTS

• **General and reference → General conference proceedings**.

KEYWORDS

Visible light communication, LiFi, OFDM, probabilistic shaping, average symbol energy, symbol error ratio

ACM Reference Format:
Tilahun Zerihun Gutema, Harald Haas, and Wasiu O. Popoola. 2020. OFDM Based Visible Light Communication with Probabilistic Shaping. In *Light Up the IoT (LIOT'20), September 21, 2020, London, United Kingdom.* ACM, New York, NY, USA, 5 pages. https://doi.org/10.1145/3412449.3412548

1 INTRODUCTION

In recent years, visible light communication (VLC) based on light emitting diode (LED) attracts tremendous interests for high-speed indoor wireless communication [10]. The availability of vast and unregulated light spectrum which is free from electromagnetic interference makes it a plausible technology to complement radio frequency (RF) based communication systems. A fully connected wireless communication system of VLC offers high-speed, inherent security, and bidirectional multiuser communication [8]. Various forms of multicarrier modulation techniques such as orthogonal frequency division multiplexing (OFDM) have been applied to achieve higher spectral efficiency [15]. The combination of high order quadrature amplitude modulation (QAM) with OFDM has proven to provide high data rates of 2-Gb/s [9] and 3-Gb/s [14] using a single LED. These impressive VLC studies all use uniformly distributed symbols. But there exists a gap to the Shannon channel capacity with uniformly distributed symbols in a noise limited channel [13].

In optical fiber communication, probabilistic shaping has been considered as means of approaching the capacity limit. It has played a crucial role for several recent record-setting optical fiber communication experiments to enhance transmission reach and capacity[2, 3, 7, 16, 17]. In probabilistic shaping, constellation points are assigned with differing probabilities which will give the constellation Gaussian-like distribution. For that, a distribution matcher such as constant composition distribution matching (CCDM) is required to allocate independent input bits into output symbols with a desired probability distribution [12].

In this workshop paper, we present a DC-biased optical OFDM based VLC system with uniformly distributed and probabilistic shaping applied on a symbol-by-symbol basis. The impact of choosing different entropy levels for probabilistically shaped symbols on average symbol energy is examined. The error performance results for both cases of uniformly distributed and probabilistic shaping are presented.

The remainder of the paper is organized as follows. In Section 2, the concept of probabilistic shaping and achievable information rate are discussed. Section 3 presents the DC-biased optical OFDM system model while Section 4 discusses the comparative average symbol energy and error performance. Finally, concluding remarks are provided in Section 5.

2 THE CONCEPT OF PROBABILISTIC SHAPING

In regular square QAM constellation, all of the constellation points are distributed uniformly. In contrast, probabilistic shaping assigns symbols with differing probabilities and shapes the probability of occurrence of the constellation points. This is realized by transmitting low energy symbols more frequently than high energy symbols and hence saves energy. Fig. 1 graphically illustrates probabilistic shaped 64-QAM for four different entropy values. It can be seen that the lower the entropy values, the higher the probability for symbols in the most inside circle of the constellation to be chosen and hence the more frequently those symbols are used.

LIOT'20, September 21, 2020, London, United Kingdom

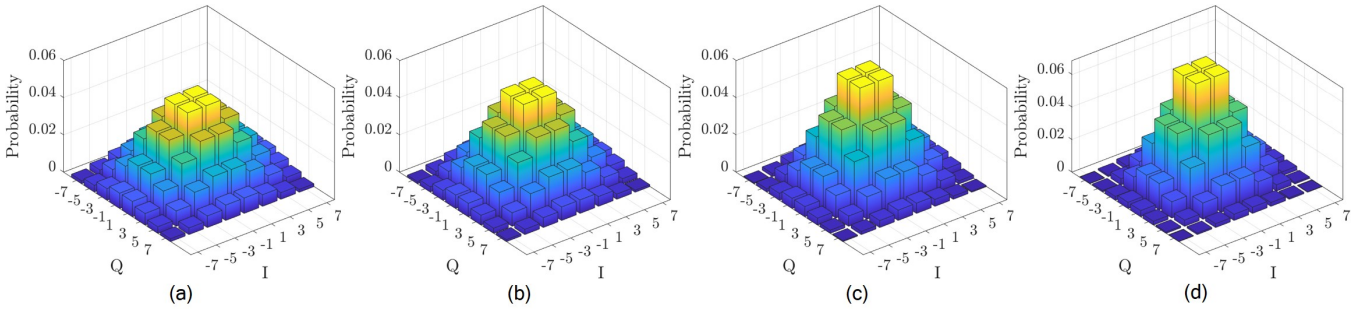

Figure 1: Graphical illustration for probabilistic shaped 64-QAM with four different entropy, $\mathbb{H}(\mathbf{X})$. (a) $\mathbb{H}(\mathbf{X})$= 5.88 bits, (b) $\mathbb{H}(\mathbf{X})$= 5.70 bits, (c) $\mathbb{H}(\mathbf{X})$= 5.40 bits, (d) $\mathbb{H}(\mathbf{X})$= 5.10 bits.

An important element to map input information bits to probabilistically shaped symbols is a distribution matcher. Constant composition distribution matcher (CCDM), proposed in [12], provides practical, invertible, fixed-to-fixed (f2f) length distribution matcher and has drawn considerable interest in application of probabilistic shaping in optical fiber communication [1–3, 5].

2.1 Achievable Information Rate Using Probabilistic Shaping

To approach Shannon's capacity limit of an additive white Gaussian noise (AWGN) channel, given the power constraint in the transmitter side, the channel must be fed by a Gaussian source [4]. This can be achieved by applying a probabilistic shaping to M-QAM symbols, which gives a Gaussian-like distribution over the input constellation. [3]. It has been shown that the best possible distribution with which to select constellation points is a Maxwell-Boltzmann distribution which gives ultimate shaping gain in any dimension [11]. In this work, we applied probabilistic shaping on a symbol-by-symbol basis and use normal distribution, with mean $\mu = 0$ and variance σ^2 to generate M-QAM symbols. The resulting entropy is given as $\mathbb{H} = \frac{1}{2}\log_2\left(2\pi e\sigma^2\right)$. For instance, for the probabilistic shaped 64-QAM shown in Fig. 1 (a), the entropy is chosen to be 5.88 bits and the σ^2 is determined from this value to be 203.067.

Consider an independent and identically distributed discrete channel input $\mathbf{X} = x_1, x_2, \ldots, x_n$. This symbol-wise input $\mathbf{X}$ is the complex M-QAM symbols with unit energy, i.e. $\mathbb{E}[|\mathbf{X}|^2] = 1$. The modulation order denoted by M takes on 2^k, where k is number of bits per symbol. We consider only the case where k is even. Thus, M-QAM has a square constellation and can be decomposed into its constituent one-dimensional $\sqrt{M}$-PAM constellation. This means that every QAM symbol can be considered as two consecutive PAM symbols that represent real and imaginary parts of the QAM symbol. The corresponding output of the channel is $\mathbf{Y} = y_1, y_2, \ldots, y_n$.

The mutual information between channel input $\mathbf{X}$ and output $\mathbf{Y}$ is defined as;

$$\mathbb{I}(\mathbf{X};\mathbf{Y}) = \mathbb{E}\left[\log_2 \frac{P_{\mathrm{Y|X}}(y|x)}{P_{\mathrm{Y}}(y)}\right], \tag{1}$$

where $P_{\mathrm{Y}}(y) = \sum_{x\in\mathbf{X}} P_{\mathrm{Y|X}}(y|x)\, P_X(x)$ is the marginal distribution of $\mathbf{Y}$, with marginal distribution of $\mathbf{X}$ denoted as $P_X(x)$ and

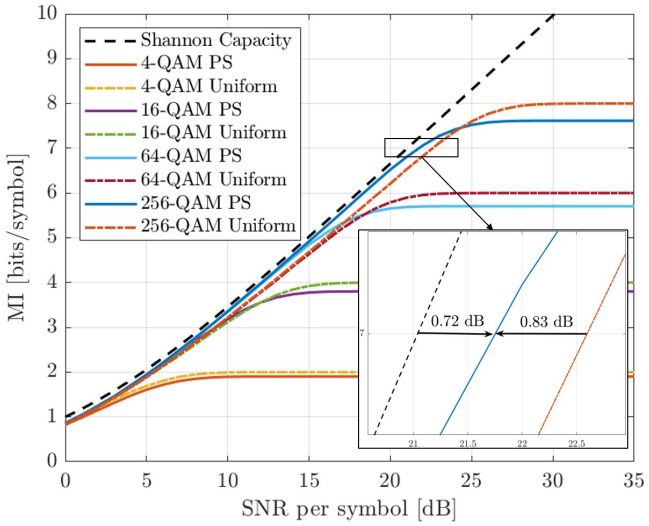

Figure 2: Mutual information with SNR per symbol, defined as a ratio of signal energy to noise power spectral density, for uniformly distributed and probabilistic shaped 4-QAM, 16-QAM, 64-QAM, and 256-QAM. The Shannon's capacity limit is shown as a reference.

$\mathbb{E}[\cdot]$ denoting expectation. The channel can be considered as memoryless, fixed auxiliary, and two-dimensional circularly symmetric and can be described by the channel conditional probability density $P_{\mathrm{Y|X}}$ [7]:

$$P_{\mathrm{Y|X}}(y|x) = \frac{1}{\sigma_n\sqrt{2\pi}} \exp\left(-\frac{|y-x|^2}{2\sigma_n^2}\right) \tag{2}$$

where σ_n^2 is the noise variance of the auxiliary channel.

To evaluate the mutual information using Eq. (1), a Monte Carlo simulations of N input-output pairs (x_k, y_k) of the channel can be used as an estimation. This gives achievable information rate in bits per symbols, $\mathrm{R_{SYM}}$ as a lower bound to the mutual information $\mathbb{I}(\mathbf{X};\mathbf{Y})$. That is:

$$\mathrm{R_{SYM}} \approx \frac{1}{N}\sum_{k=1}^{N} \log_2 \frac{P_{Y|X}(y_k|x_k)}{P_Y(y_k)}. \tag{3}$$

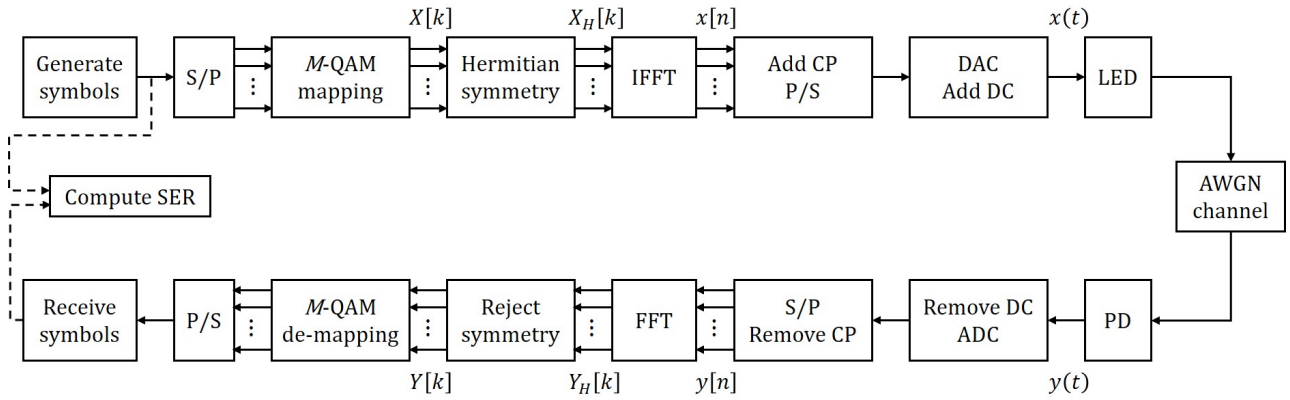

Figure 3: A block diagram illustration of DC-biased optical OFDM communication system.

In Fig. 2, the simulation result of mutual information in bits per symbol of Eq. (3) is depicted. For probabilistic shaped symbols, the entropy used in the simulation for 4-QAM, 16-QAM, 64-QAM, and 256-QAM is 1.9, 3.8, 5.7, and 7.6 bits, respectively. The Shannon's capacity limit $C = \log_2(1 + \text{SNR})$ is also shown as a reference. As shown in the figure, as the SNR increases, the mutual information of 4-QAM, 16-QAM, 64-QAM, and 256-QAM, for both uniformly distributed and probabilistic shaped, saturate to 2, 4, 6, and 8 bits/symbol, respectively. The gain in probabilistic shaping in each of these modulation orders can be seen in the regions where the SNR per symbol is lower than the SNR threshold where the mutual information starts to saturate. That is, in the low SNR regime, the mutual information of a probabilistic shaped symbols approaches the Shannon capacity limit. To illustrate, the inset in Fig. 2 shows that at 7 bits/symbol mutual information, 0.83 dB can be gained from probabilistic shaping over the uniformly distributed symbols while the gap to the Shannon limit with the probabilistically shaped symbols is 0.72 dB.

3 OPTICAL OFDM COMMUNICATION SYSTEM SIMULATION

A DC-biased optical OFDM based optical communication system block diagram is shown in Fig. 3. In this system, we start by generating random symbols. For comparison purpose we consider both uniformly distributed symbols and probabilistic shaped symbols. These symbols are then mapped in parallel onto M-QAM constellation points $X[k]$, where $k = 0, 1, \ldots, N_{DSC} - 1$ and N_{DSC} being the number of data subcarriers. To generate real value signals in time domain, Hermitian symmetry is applied to the frame prior to the IFFT operation. The symmetry signal specifies the following conditions:

$$X_H[k] = \left[0, X(1), \ldots, X(N_{DSC} - 1), 0, X^*(N_{DSC} - 1), \ldots, X^*(1)\right] \tag{4}$$

where $k = 0, 1, \ldots, N_{SC} - 1$, $N_{SC} = 2(N_{DSC} + 1)$, and $[\cdot]^*$ denotes the complex conjugate operator. After the operation of IFFT, the time-domain samples are given as

$$x[n] = \frac{1}{N_{SC}} \sum_{m=0}^{N_{SC}-1} X_H[m] \exp\left(\frac{\mathrm{j}2\pi nm}{N_{SC}}\right), \qquad 0 \le n \le N_{SC} - 1. \tag{5}$$

The time domain sample is then converted into serial and a cyclic prefix (CP) is added onto it to act as a guard band between successive OFDM frames and overcome intersymbol and intercarrier interference in dispersive (multipath propagation) optical wireless channel. The discrete sampled signal $x[n]$ is then fed into digital-to-analog (DAC) converter to obtain a continuous time-domain signal $x_a(t)$. To ensure unipolar time domain signal required for intensity modulation of the optical source (LED in this case), a DC bias x_{DC} is added. The condition $x_{DC} \ge |\min(x_a(t))|$ must be met to ensure the signal, $x(t)$ is unipolar signal.

The real unipolar time-domain signal $x(t)$ is then used to drive the LED. We consider two types of white LEDs which are warm white LED and cool white LED. We model the response of the LEDs as a low-pass filter. It has been shown that warm white LEDs can be modelled as a first-order LPF and cool white LEDs as a third-order LPF [6].

At the receiver, the reverse operation to that of the transmitter side is done. The photodetector converts the optical signal back to electrical signal. The DC added in the transmitted is then removed before the time-domain continuous signal is sampled by analog-to-digital converter (ADC). Afterwards, the CP are removed and framed together in parallel. An FFT operation transforms the received signal $y(t)$ into its frequency domain equivalent $Y[k]$ and the Hermitian symmetry component removed prior to M-QAM de-mapping. The M-QAM de-mapper perform QAM demodulation to estimate the transmitted symbols. From this, symbol error ratio of the system is evaluated by comparing the transmitted symbol with the received symbols.

4 RESULTS AND DISCUSSION

The DC-biased optical OFDM block diagram shown in Fig. 3 is simulated for both uniformly distributed and probabilistic shaped symbols. We consider 4-QAM, 16-QAM, 64-QAM, and 256-QAM. For probabilistic shaping, for the purpose of illustrating the effect of

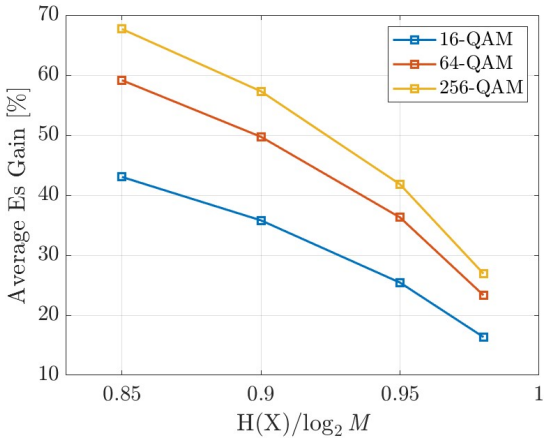

Figure 4: The gain in average symbol energy for different entropy of probabilistic shaped symbols over uniformly distributed for 16-QAM, 64-QAM, and 256-QAM.

different values of entropy, we consider four scenarios i.e. $\mathbb{H}(\mathbf{X}) = \{0.85, 0.90, 0.95, 0.98\} \times \log_2 M$ with modulation order $M = 4, 16, 64, 256$.

4.1 Average Symbol Energy

To evaluate the gain in the average transmitted symbol energy of M-QAM signal, the symbol energy of uniformly distributed symbols is compared with that of the probabilistically shaped symbols for the aforementioned four scenarios. The simulation results in Fig. 4 show that 256-QAM gives a larger gain in average symbol energy compared to other QAM constellations. This is due to the fact that lower energy symbols are used more frequently as illustrated in Fig. 1. Furthermore, the gain is higher in lower entropy scenarios. These results are expected as probabilistic shaping has more constellation shaping effect as the modulation order increases and in lower entropy, as well.

4.2 Symbol Error Ratio Performance

In this section, symbol error ratio comparison between uniformly distributed symbols and probabilistic shaped symbols is presented. In the simulations, 128 OFDM data-carrying subcarrier are used. The LED is modelled as a first-order LPF with a -3 dB cut-off frequency of 10 MHz and the sampling rate is taken as 20 MSa/s. The scenario with an entropy of $0.98 \times \log_2 M$ is chosen for probabilistic shaped symbol. Fig. 5 shows the comparison in symbol error ratio between uniformly distribution and probabilistic shaping for different modulation orders. The theoretical symbol error ratio for uniformly distributed symbols in AWGN channel is also shown as a reference. For 4-QAM, as all four symbols are in a single constellation ring, there is no gain from using probabilistic shaping in symbols error ratio and hence it is not shown here. However, with higher modulation orders probabilistic shaping outperforms uniform distribution. This is shown in Fig. 5 (a), (b), and (c) for 16-QAM, 64-QAM, and 256-QAM, respectively. For achieving a symbol error ratio of 10^{-3}, 2.1 dB, 2.6 dB, 3 dB improvement is obtained in SNR per symbol for 16-QAM, 64-QAM, and 256-QAM respectively.

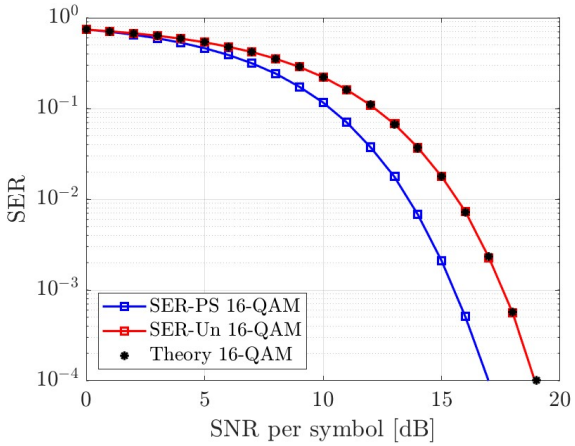

(a)

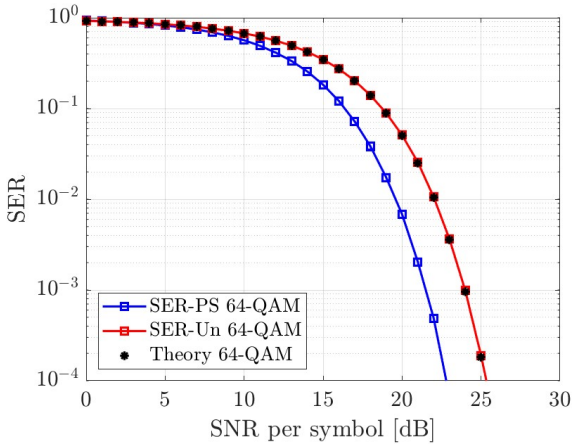

(b)

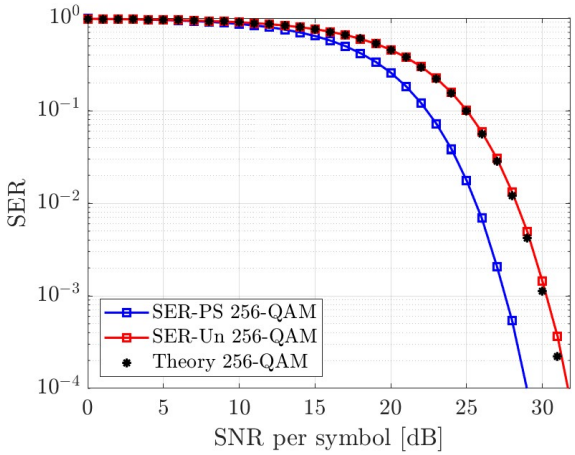

(c)

Figure 5: Symbol error ratio (SER) with SNR per symbol for uniformly distributed and probabilistic shaped 16-QAM, 64-QAM, and 256-QAM using 3.92, 5.88, and 7.84 bits as entropy, respectively. The theoretical symbols error ratio is shown as a reference.

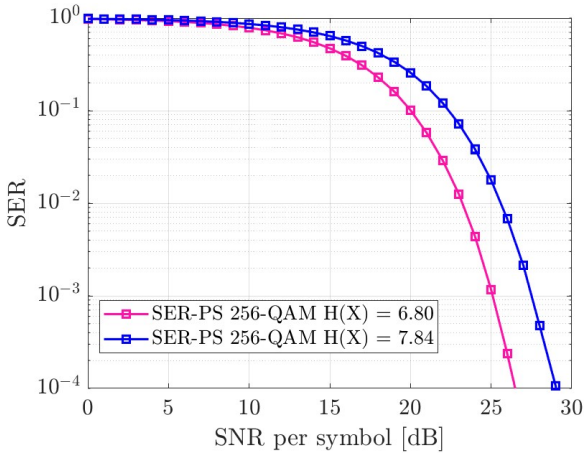

Figure 6: Symbol error ratio with SNR per symbol for probabilistic shaped 256-QAM using 6.80 and 7.84 bits as entropy.

The error performance gain increases at lower entropy values for the probabilistically shaped symbols. This is shown in Fig. 6 for probabilistic shaped 256-QAM with entropy values of 6.80 bits and 7.84 bits. For the same symbol error ratio of 10^{-3}, the lower entropy probabilistic shaping improves the gain by almost 2.5 dB. This energy saving makes probabilistic shaping very attractive for VLC in different scenarios, including underwater optical communication.

5 CONCLUSION

In this work, we have studied probabilistic shaping for DC-biased optical OFDM system. It has been shown that with probabilistic shaped 256-QAM and entropy of 6.8 bits, an average symbol energy reduction of up to 70% could be obtained relative to uniformly distributed 256-QAM. In terms of error rate, the probabilistic shaped M-QAM outperforms the uniformly distributed M-QAM in noise limited channel conditions. For probabilistically shaped 256-QAM with an entropy of 7.84 bits, we have shown 3 dB gain in SNR per symbol compared to uniform 256-QAM at a symbol error ratio of 10^{-3}. This gain is increased to 5.5 dB by decreasing the entropy to 6.80 bits.

ACKNOWLEDGMENTS

This work is funded by the European Union H2020-MSCA-ITN-2018 №: 814215 grant titled ENLIGHT'EM: European Training Network in Low-Energy Visible Light IoT Systems; https://enlightem.eu/.

REFERENCES

[1] Georg Böcherer, Fabian Steiner, and Patrick Schulte. 2015. Bandwidth efficient and rate-matched low-density parity-check coded modulation. *IEEE Transactions on Communications* 63, 12 (2015), 4651–4665.

[2] Fred Buchali, Georg Böcherer, Wilfried Idler, Laurent Schmalen, Patrick Schulte, and Fabian Steiner. 2015. Experimental demonstration of capacity increase and rate-adaptation by probabilistically shaped 64-QAM. In *2015 European Conference on Optical Communication (ECOC)*. IEEE, 1–3.

[3] Fred Buchali, Fabian Steiner, Georg Böcherer, Laurent Schmalen, Patrick Schulte, and Wilfried Idler. 2016. Rate adaptation and reach increase by probabilistically shaped 64-QAM: An experimental demonstration. *Journal of Lightwave Technology* 34, 7 (2016), 1599–1609.

[4] Di Che and William Shieh. 2017. Entropy-loading: multi-carrier constellation-shaping for colored-SNR optical channels. In *2017 Optical Fiber Communications Conference and Exhibition (OFC)*. IEEE, 1–3.

[5] Junho Cho and Peter J Winzer. 2019. Probabilistic constellation shaping for optical fiber communications. *Journal of Lightwave Technology* 37, 6 (2019), 1590–1607.

[6] Guler Egecan, Kabiru O Akande, Paul Anthony Haighy, and Wasiu O Popoola. 2018. Frequency Response Modelling of Cool and Warm White LEDs in VLC Systems. In *Proceedings of First Western Conference on Wireless Telecommunications Wireless Asia Pacific*. Iran, 63–66. https://www.civilica.com/Paper-WACOWC01-WACOWC01_010.html

[7] Tobias Fehenberger, Alex Alvarado, Georg Böcherer, and Norbert Hanik. 2016. On probabilistic shaping of quadrature amplitude modulation for the nonlinear fiber channel. *Journal of Lightwave Technology* 34, 21 (2016), 5063–5073.

[8] Harald Haas, Liang Yin, Yunlu Wang, and Cheng Chen. 2015. What is lifi? *Journal of lightwave technology* 34, 6 (2015), 1533–1544.

[9] Xingxing Huang, Siyuan Chen, Zhixin Wang, Jianyang Shi, Yiguang Wang, Jiangnan Xiao, and Nan Chi. 2015. 2.0-Gb/s visible light link based on adaptive bit allocation OFDM of a single phosphorescent white LED. *IEEE Photonics Journal* 7, 5 (2015), 1–8.

[10] Dilukshan Karunatilaka, Fahad Zafar, Vineetha Kalavally, and Rajendran Parthiban. 2015. LED based indoor visible light communications: State of the art. *IEEE Communications Surveys & Tutorials* 17, 3 (2015), 1649–1678.

[11] Frank R Kschischang and Subbarayan Pasupathy. 1993. Optimal nonuniform signaling for Gaussian channels. *IEEE Transactions on Information Theory* 39, 3 (1993), 913–929.

[12] Patrick Schulte and Georg Böcherer. 2015. Constant composition distribution matching. *IEEE Transactions on Information Theory* 62, 1 (2015), 430–434.

[13] Claude E Shannon. 1948. A mathematical theory of communication. *Bell system technical journal* 27, 3 (1948), 379–423.

[14] Dobroslav Tsonev, Hyunchae Chun, Sujan Rajbhandari, Jonathan JD McKendry, Stefan Videv, Erdan Gu, Mohsin Haji, Scott Watson, Anthony E Kelly, Grahame Faulkner, et al. 2014. A 3-Gb/s Single-LED OFDM-Based Wireless VLC Link Using a Gallium Nitride μLED. *IEEE Photonics Technology Letters* 26, 7 (2014), 637–640.

[15] Dobroslav Tsonev, Stefan Videv, and Harald Haas. 2015. Unlocking spectral efficiency in intensity modulation and direct detection systems. *IEEE Journal on Selected Areas in Communications* 33, 9 (2015), 1758–1770.

[16] Metodi P Yankov, Francesco Da Ros, Edson P da Silva, Søren Forchhammer, Knud J Larsen, Leif K Oxenløwe, Michael Galili, and Darko Zibar. 2016. Constellation shaping for WDM systems using 256QAM/1024QAM with probabilistic optimization. *Journal of Lightwave Technology* 34, 22 (2016), 5146–5156.

[17] Metodi P Yankov, Darko Zibar, Knud J Larsen, Lars PB Christensen, and Søren Forchhammer. 2014. Constellation shaping for fiber-optic channels with QAM and high spectral efficiency. *IEEE Photonics Technology Letters* 26, 23 (2014), 2407–2410.